

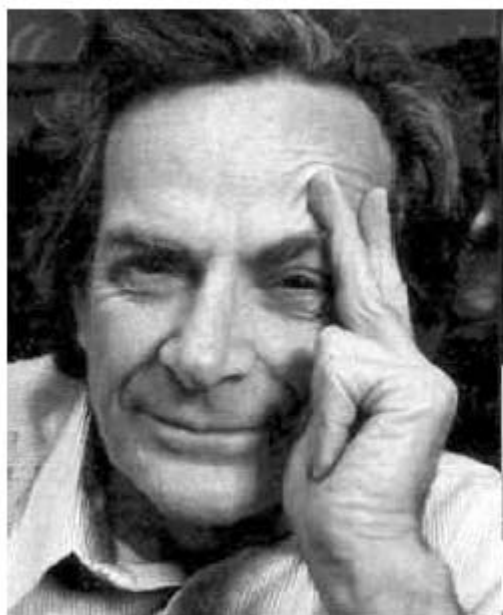
Brief Introduction to Photonic Crystals

ByoungHo Lee
School of Electrical Engineering
Seoul National University

byoungho@snu.ac.kr



Nano



**“There is Plenty
of Room at the
Bottom”**

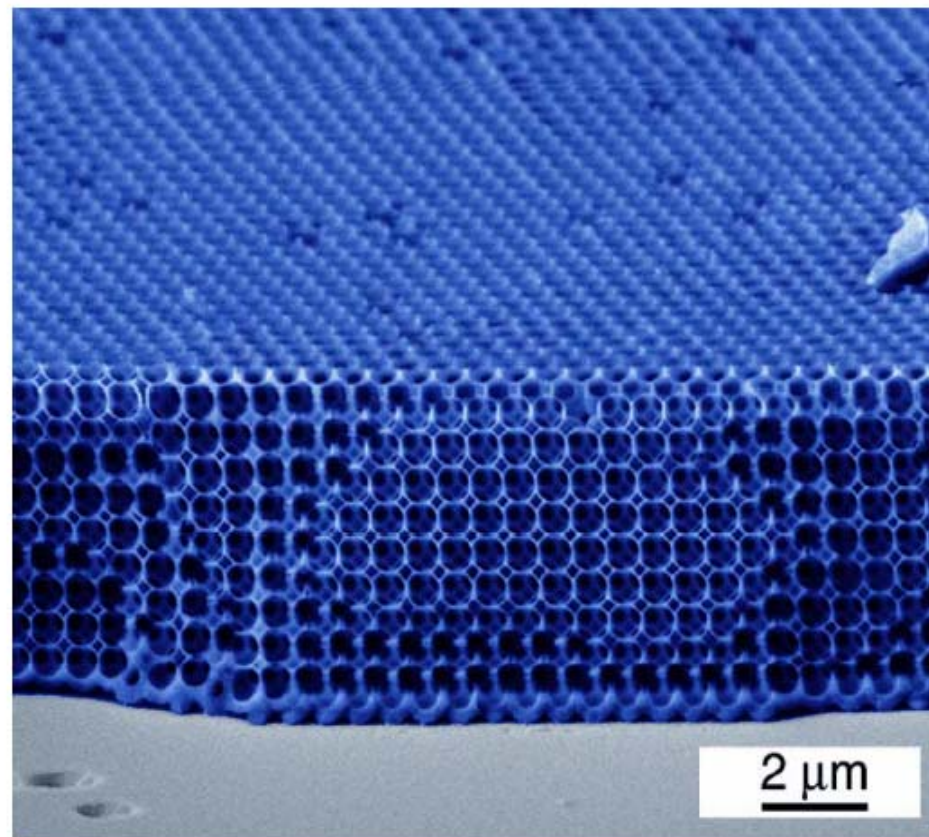
Prof. Richard P. Feynman

December, 1959

California Institute of Technology

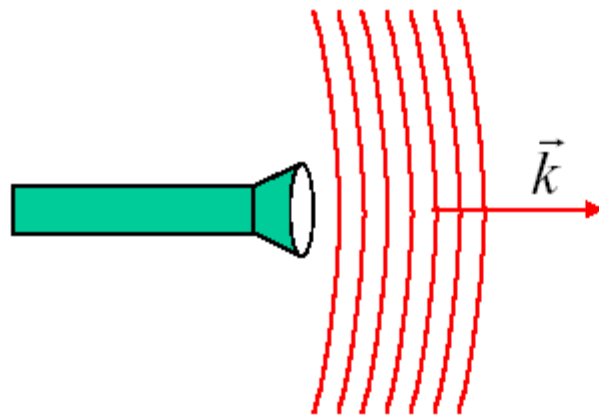
<http://www.zyvex.com/nanotech/feynman.html>

Photonic crystals



[Y. A. Vlasov *et al.*, *Nature* **414**, 289 (2001).]

Scattering



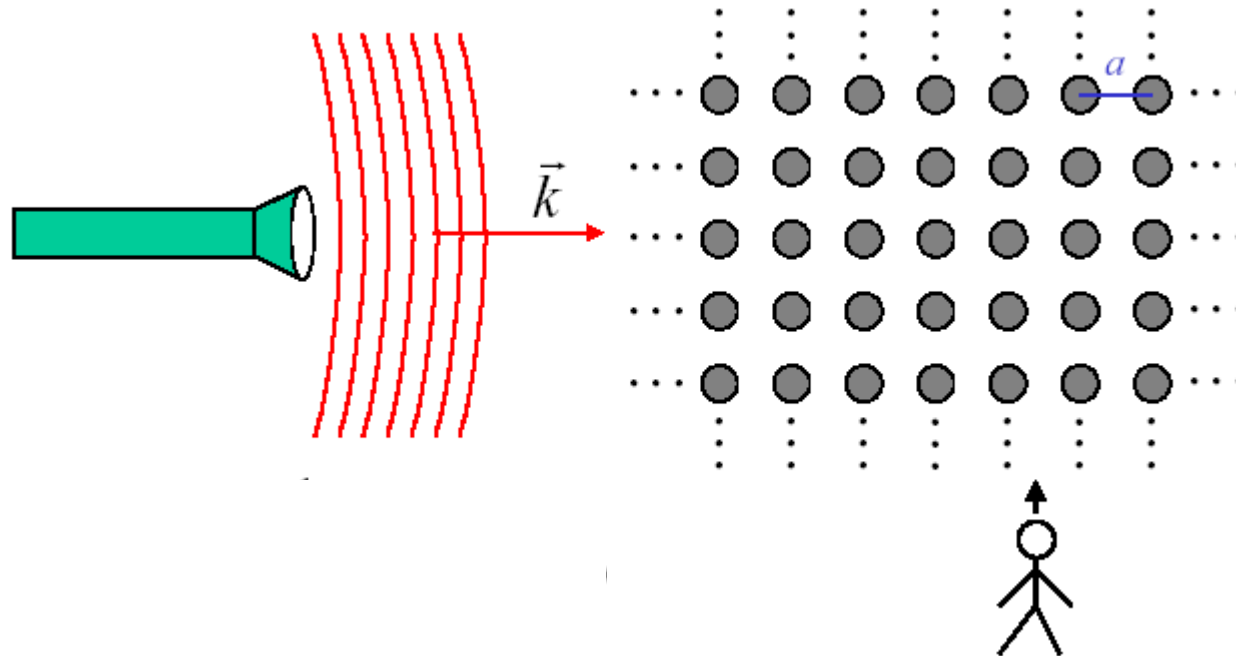
planewave

$$\vec{E}, \vec{H} \sim e^{i(\vec{k} \cdot \vec{x} - \omega t)}$$

$$|\vec{k}| = \omega / c = \frac{2\pi}{\lambda}$$



Periodic medium



No light propagation for certain wavelengths:
a photonic bandgap

Photonic structures in biology

Pete Vukusic and J. Roy Sambles

Thin Film Photonics, School of Physics, Exeter University, Exeter EX44QL, UK (e-mail: P.Vukusic@ex.ac.uk)

Millions of years before we began to manipulate the flow of light using synthetic structures, biological systems were using nanometre-scale architectures to produce striking optical effects. An astonishing variety of natural photonic structures exists: a species of Brittlestar uses photonic elements composed of calcite to collect light, *Morpho* butterflies use multiple layers of cuticle and air to produce their striking blue colour and some insects use arrays of elements, known as nipple arrays, to reduce reflectivity in their compound eyes. Natural photonic structures are providing inspiration for technological applications.

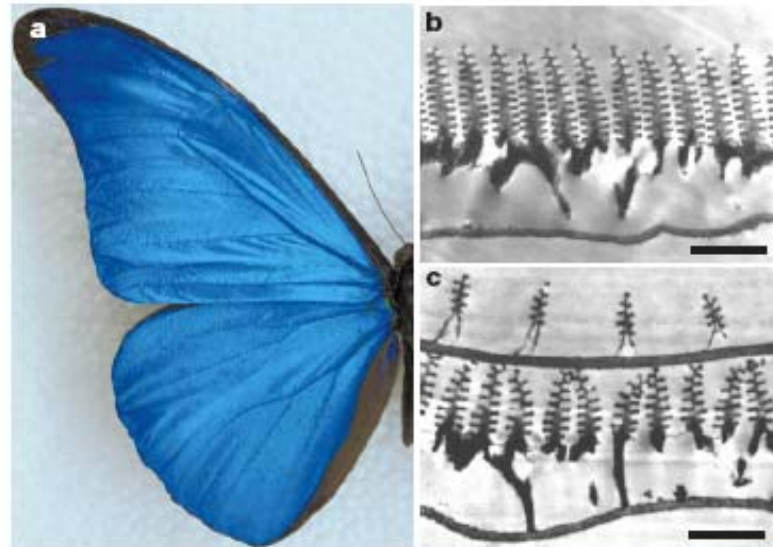
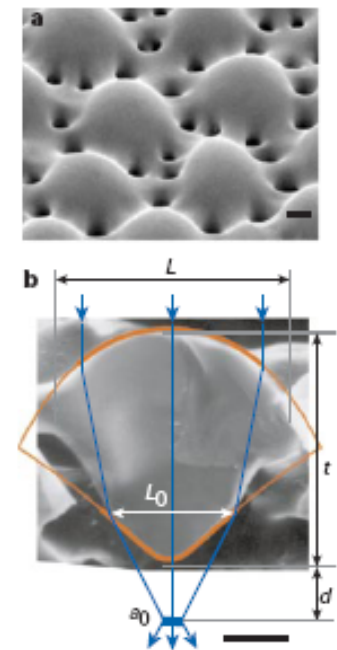


Figure 3 Iridescence in the butterfly *Morpho rhetenor*. **a**, Real colour image of the blue iridescence from a *M. rhetenor* wing. **b**, Transmission electron micrograph (TEM) images showing wing-scale cross-sections of *M. rhetenor*. **c**, TEM images of a wing-scale cross-section of the related species *M. didius* reveal its discretely configured multilayers. The high occupancy and high layer number of *M. rhetenor* in **b** creates an intense reflectivity that contrasts with the more diffusely coloured appearance of *M. didius*, in which an overlying second layer of scales effects strong diffraction⁴. Bars, **a**, 1 cm; **b**, 1.8 μm ; **c**, 1.3 μm .

tonic
the
f life
or an
lence
dator
ems,
an be
rtain
ty of
oday.
ature

truc-
ray in
were
layer
nent
y fish
many
that
est in
es of

Figure 1 Peripheral layer of ophiocomid brittlestars. **a**, Scanning electron micrographs (SEM) of the peripheral layer of a dorsal arm plate from the brittlestar *Ophiocoma wendtii* showing the microlens array **b**, SEM of an individual lens in *O. wendtii*. The functional region of this lens (L_f) closely matches the profile of a lens that is compensated for spherical aberration (represented by the red lines). The light paths are shown in blue (images reproduced with permission from J. Aizenberg). Bars, 10 μm .



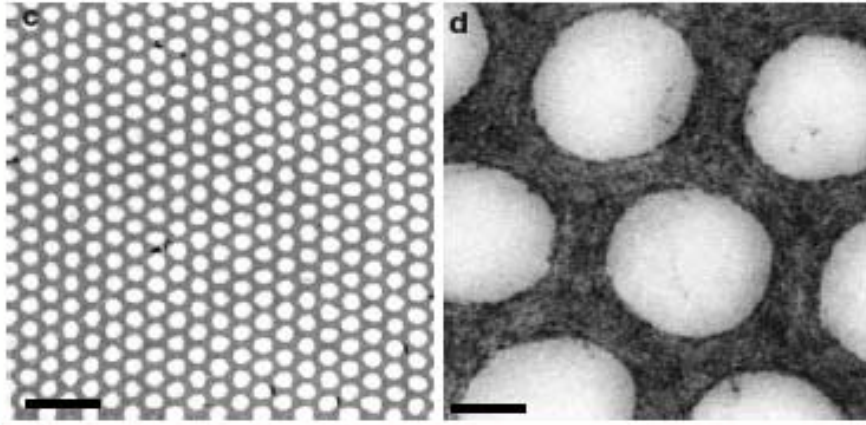
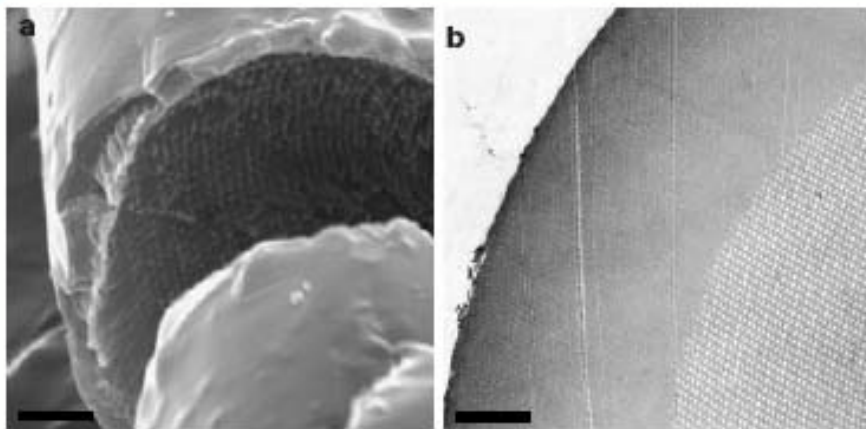


Figure 2 Iridescent setae from polychaete worms. **a**, Scanning electron micrograph (SEM) and **b–d**, transmission electron micrograph (TEM) images of transverse sections through a single iridescent seta. Bars, **a**, 2 μm ; **b**, 5 μm ; **c**, 1 μm ; **d**, 120 nm.

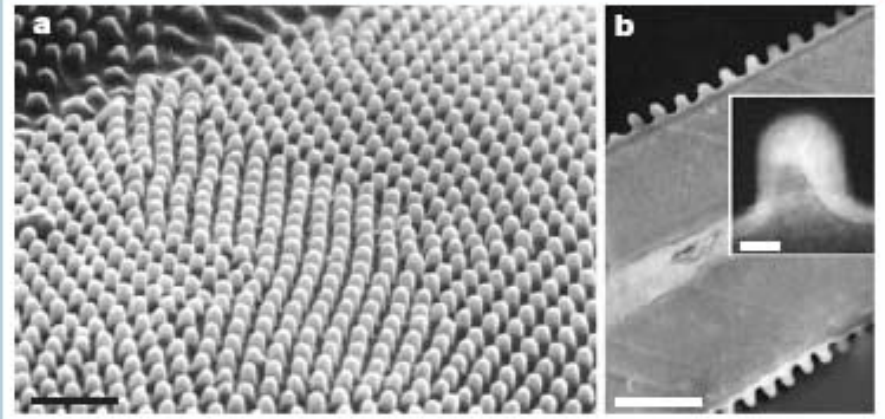


Figure 7 Anti-reflective nipple arrays. **a**, The anti-reflective nipple arrays on

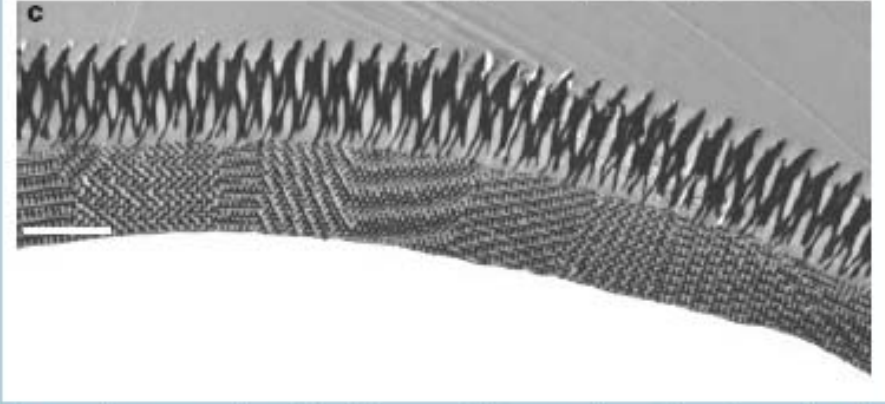
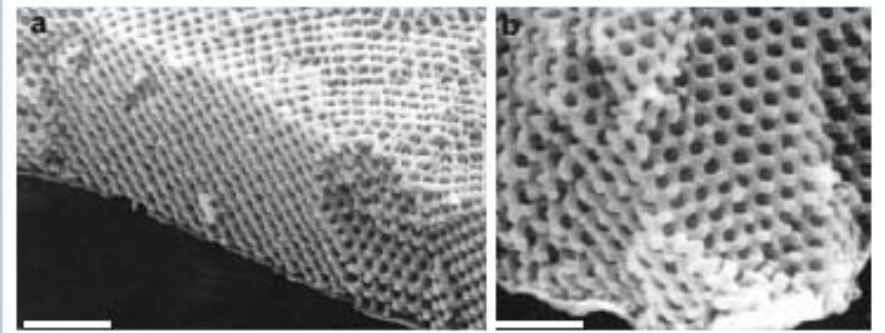
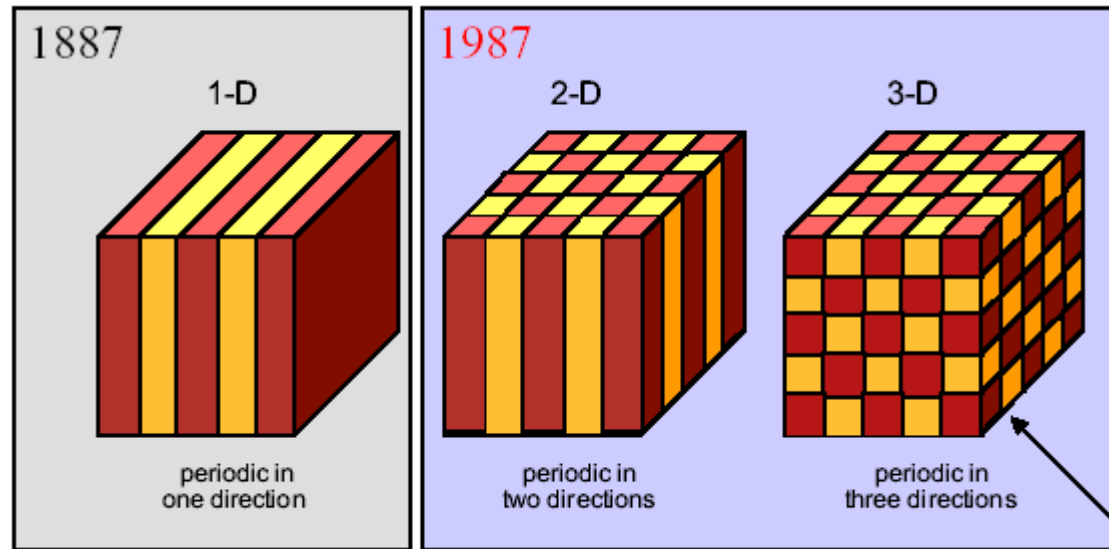


Figure 6 The green colour of *Parides sesostris* is created by a photonic crystal. **a**, **b**,

Photonic crystals

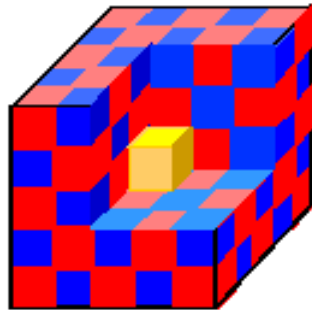


requires complex topology

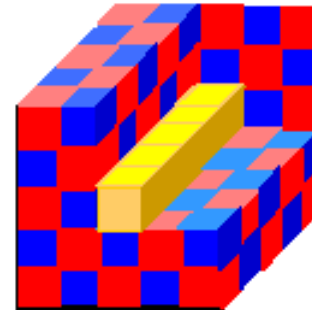
Periodic electromagnetic media

Photonic bandgap: optical insulator

Photonic crystals



Light cavities

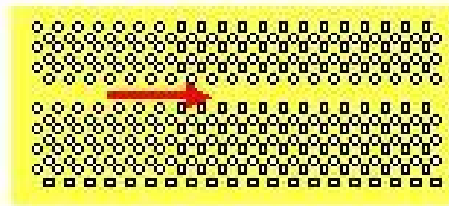


Light waveguides
(‘wires’)

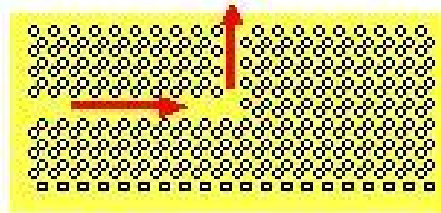
Periodic electromagnetic media

Photonic bandgap: optical insulator

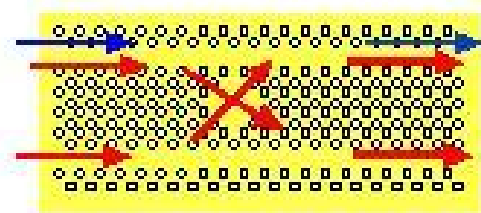
Photonic bandgap waveguides



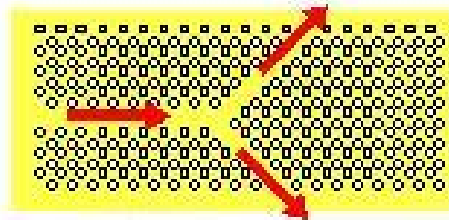
(a)



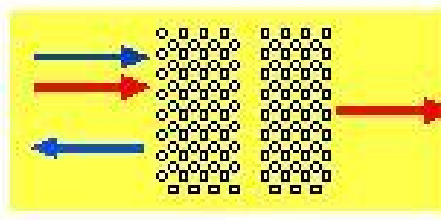
(b)



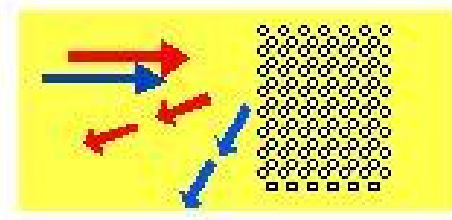
(c)



(d)



(e)



(f)

a : guide

b : sharp bend

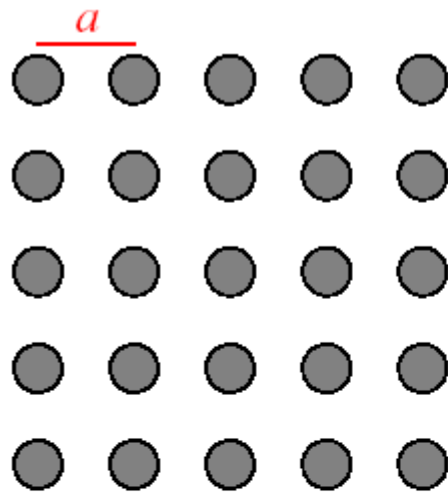
c : add/drop

d : Y-coupler

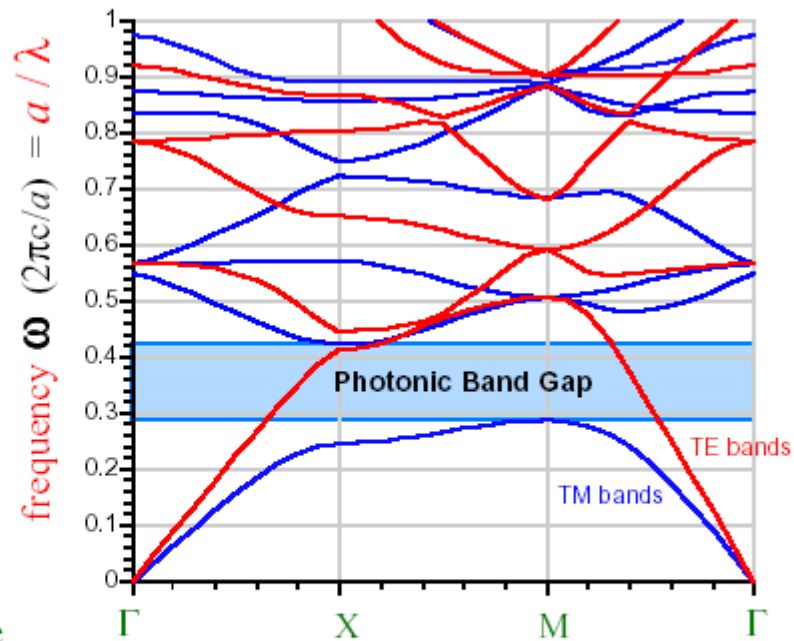
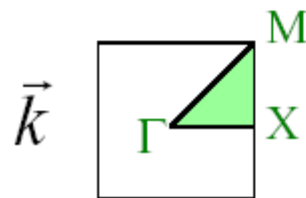
e : filter

f : dispersive element

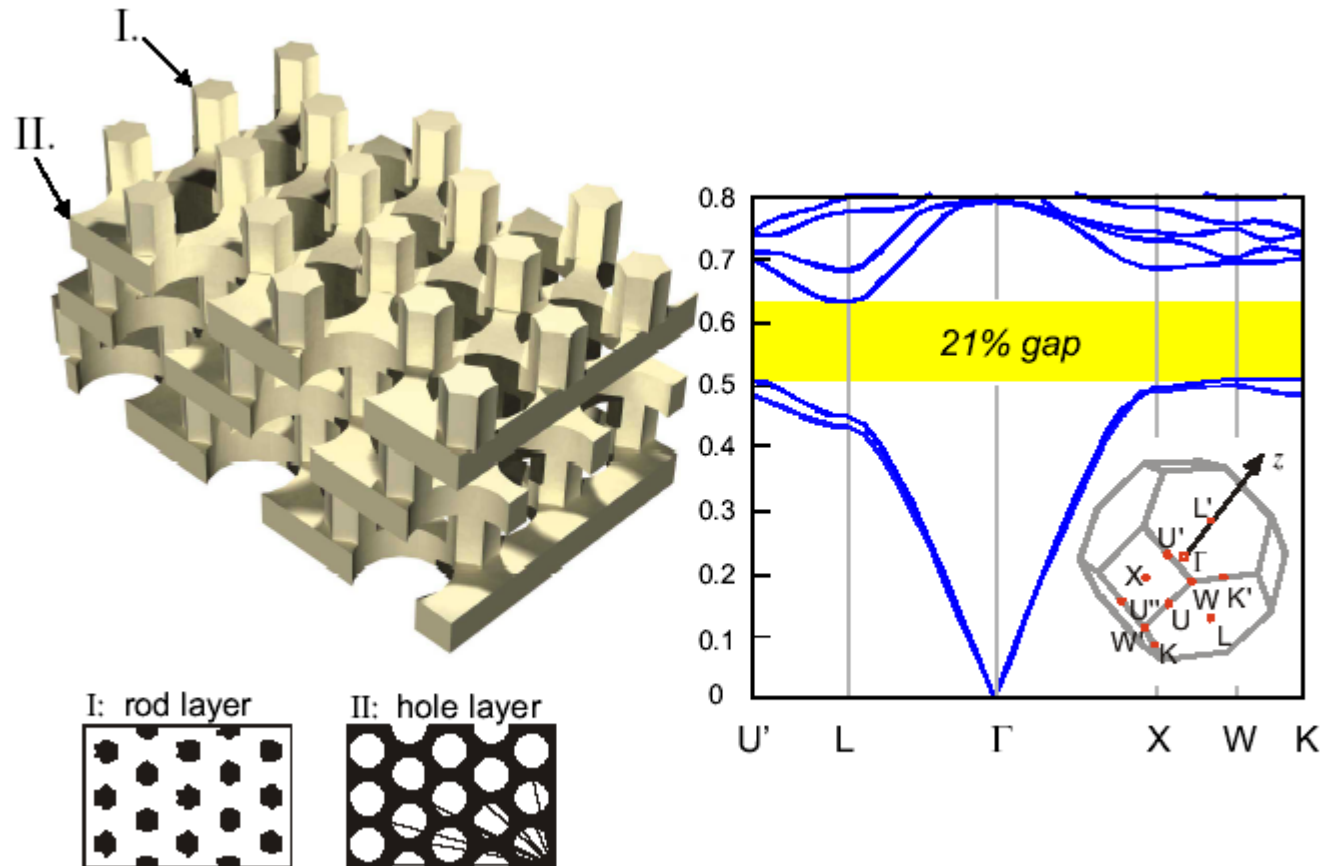
Photonic bands



irreducible Brillouin zone

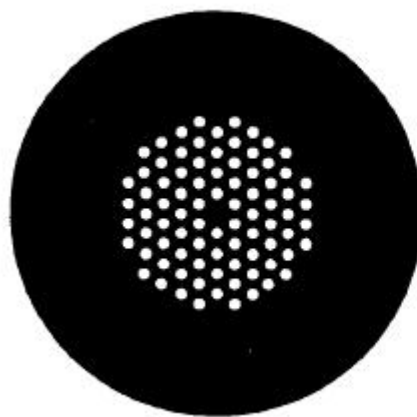


3D photonic crystals – photonic bandgap

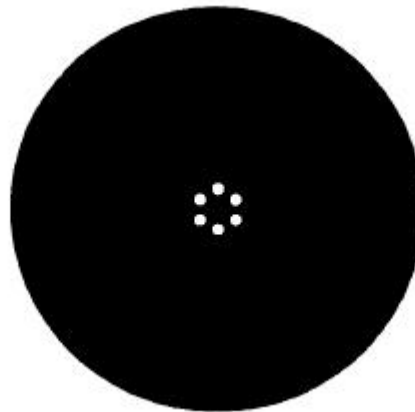


[S. G. Johnson *et al.*, *Appl. Phys. Lett.* 77, 3490 (2000)]

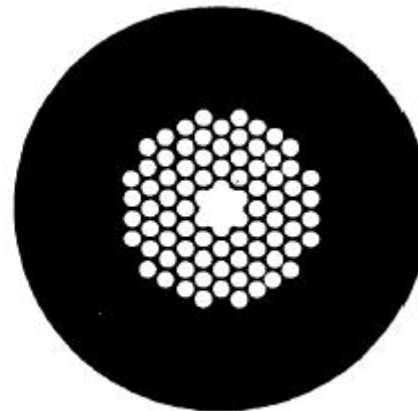
Photonic crystal fibers



(a)



(b)



(c)

a : PCF (TIR) \Leftarrow very strong core-cladding index contrast enhanced

\Leftarrow (ESM) \Leftarrow large bending loss

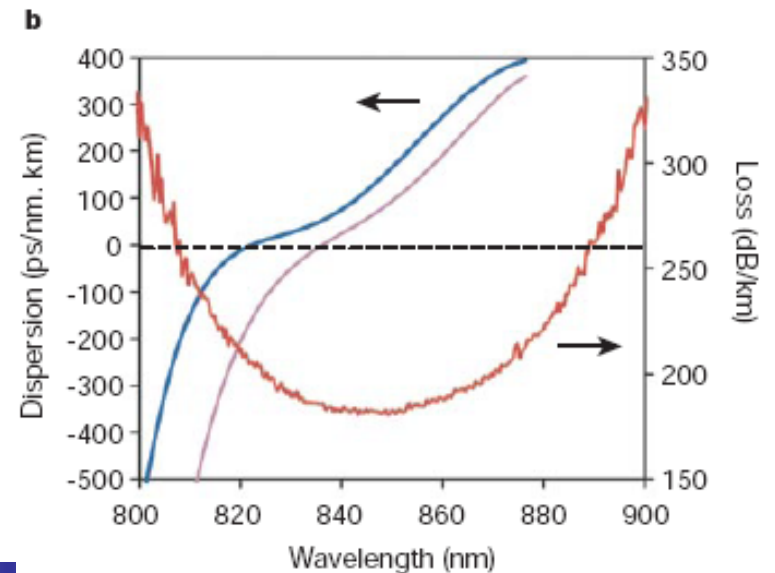
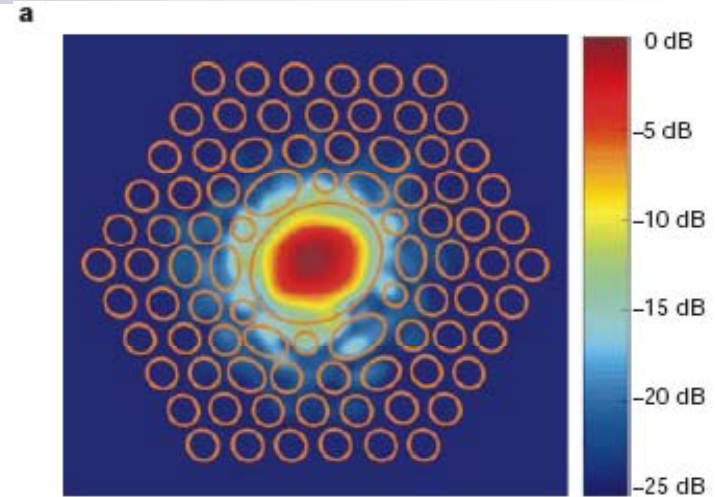
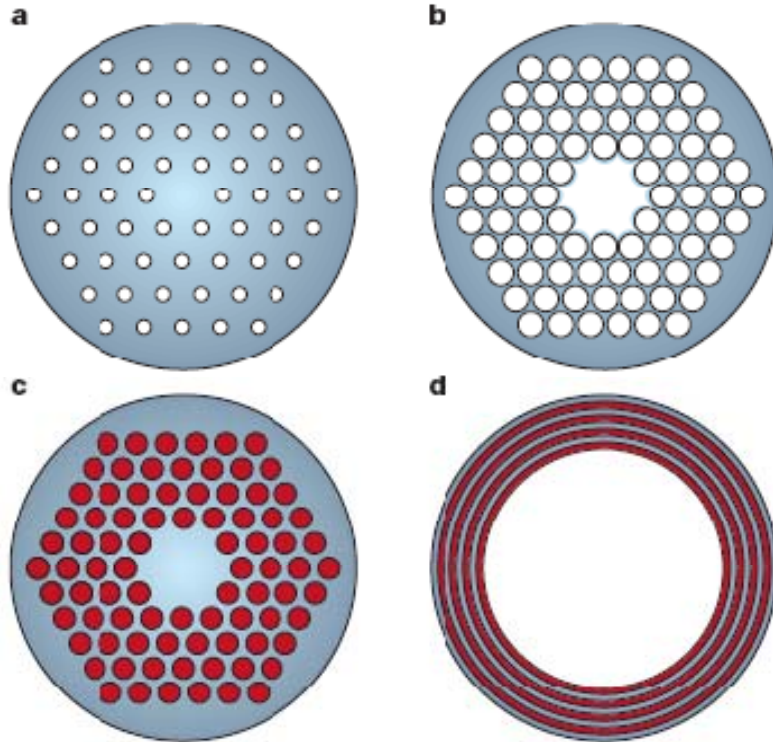
b : Air-clad core \Leftarrow highly dispersive \Leftarrow DCF

c : PBGF \Leftarrow too lossy (~ 1 dB/m) \Leftarrow still has a potential for the future

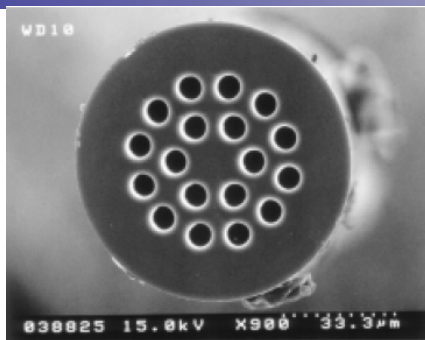
Photonic crystal fibers

Photonic crystal fibers

J. C. Knight, *Nature*, 424, pp. 847-851, 2003.

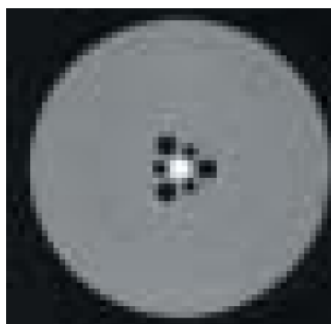


Holey fibers



Mitsubishi Cable

클래딩 지름	80 μ m
유효 코어 모드 지름	11.5 μ m
전송 손실 (1550nm)	0.35dB/km
허용 곡률 반경	7.5mm
벤딩 손실 (1550nm) ϕ 15mm \times 10 turn	<0.1dB



Fujikura

FutureGuide[®]-SR15
→ 허용 곡률 반경 15 mm

FutureGuide[®]-SR7.5
→ 허용 곡률 반경 7.5 mm

Vectorial diffractive optics

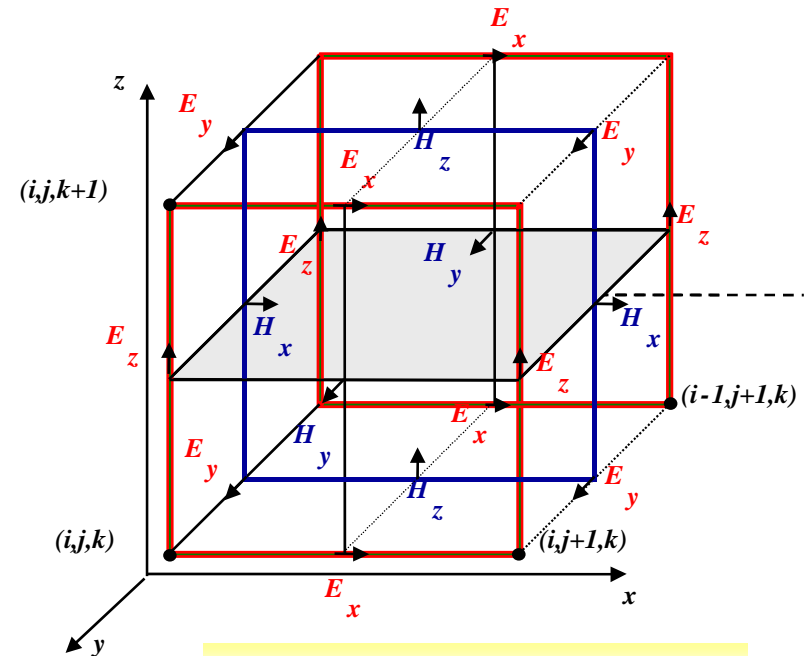
- ❑ Concepts of Maxwell equation analysis
FDTD, RCWA, PFMA
- ❑ Surface plasmon analysis
Surface plasmon resonance, excitation by finite beam
and pulses, 3D metallic structures
- ❑ Photonic crystal analysis



Finite-difference time-domain (FDTD) method

FDTD is a rigorous analysis method with widely applications from nano- to all length-scales using the Maxwell's equations and curl equations

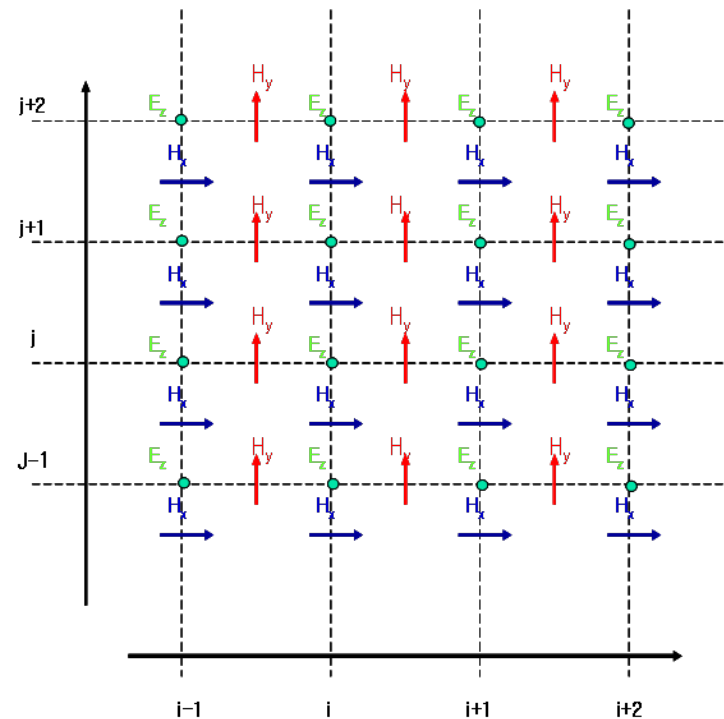
$$\begin{aligned} \frac{\partial E_x}{\partial t} &= \frac{1}{\epsilon_x} \left(\frac{\partial H_y}{\partial z} - \frac{\partial H_z}{\partial y} - \sigma_x E_x \right) & \frac{\partial H_x}{\partial t} &= \frac{1}{\mu_x} \left(\frac{\partial E_y}{\partial z} - \frac{\partial E_z}{\partial y} - \sigma_x^* H_x \right) \\ \frac{\partial E_y}{\partial t} &= \frac{1}{\epsilon_y} \left(\frac{\partial H_z}{\partial x} - \frac{\partial H_x}{\partial z} - \sigma_y E_y \right) & \frac{\partial H_y}{\partial t} &= \frac{1}{\mu_y} \left(\frac{\partial E_z}{\partial x} - \frac{\partial E_x}{\partial z} - \sigma_y^* H_y \right) \\ \frac{\partial E_z}{\partial t} &= \frac{1}{\epsilon_z} \left(\frac{\partial H_x}{\partial y} - \frac{\partial H_y}{\partial x} - \sigma_z E_z \right) & \frac{\partial H_z}{\partial t} &= \frac{1}{\mu_z} \left(\frac{\partial E_x}{\partial y} - \frac{\partial E_y}{\partial x} - \sigma_z^* H_z \right) \end{aligned}$$



3D Yee's cell geometry

Finite-difference time-domain (FDTD) method

2D Yee's cell : interleaving mesh



$$\frac{D_z^{n+0.5}(i, j) - D_z^{n-0.5}(i, j)}{\Delta t} = c_0 \left(\frac{H_y^n(i+0.5, j) - H_y^n(i-0.5, j)}{\Delta x} \right) - c_0 \left(\frac{H_x^n(i, j+0.5) - H_x^n(i, j-0.5)}{\Delta x} \right)$$

$$\frac{H_x^{n+1}(i, j+0.5) - H_x^n(i, j+0.5)}{\Delta t} = -c_0 \left(\frac{E_z^{n+0.5}(i, j+1) - E_z^{n+0.5}(i, j)}{\Delta x} \right)$$

Finite-difference time-domain (FDTD) method

- Numerical methods for EM wave solution
 - ✓ Numerical methods for solving the electromagnetic wave propagation problems
 - FEM, MOM, BPM, TLM, FDTD (which is the most popular)
 - Yee used centered finite-difference expressions for the space and time derivatives that are both simply programmed and have second-order accuracy in the space and time increments.
 - ✓ Advantages of FDTD
 - Problems exhibiting complex structures
 - Only one computation is required to get the frequency domain results over a large frequency spectrum.
 - FDTD method does not need to solve any integral and matrix equations.
 - It is conceptually simple and simple to code.
 - It is applicable to a large class of problems.
 - However, it needs very large computer memories.
 - ✓ FDTD conditions and properties
 - Stability, dispersion, source conditions, absorbing boundary conditions



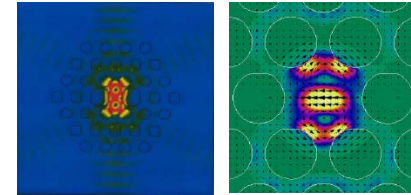
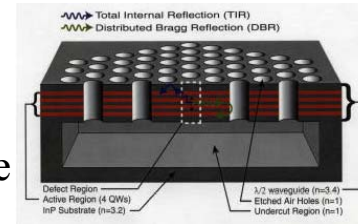
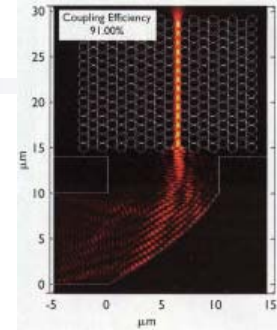
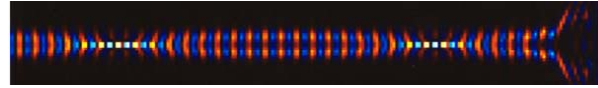
Finite-difference time-domain (FDTD) method

□ FDTD applications

✓ Waveguides and nano-photonics

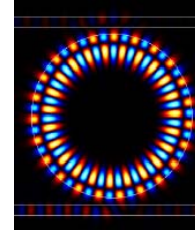
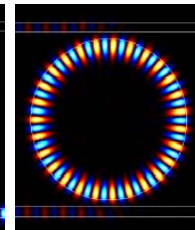
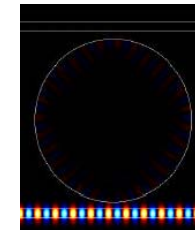
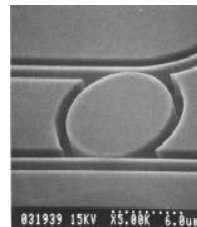
- Solitons

- Mingaleev and Kivshar, *Optics and Photonics News*, July 2002.
- Prather, *Optics and Photonics News*, June 2002.



- Defect cavities and defect mode lasers

- Painter et al., *Science*, June 11, 1999.

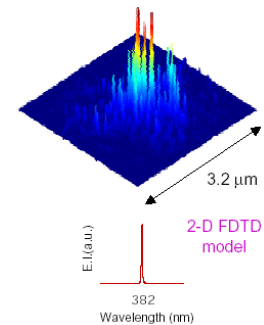
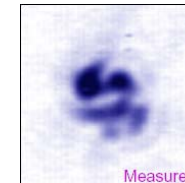
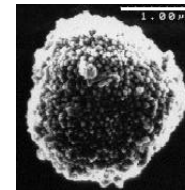


- Waveguides coupled to disks and rings

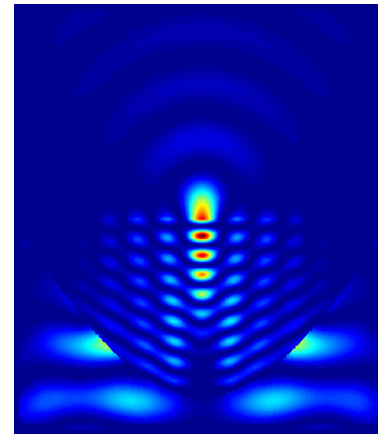
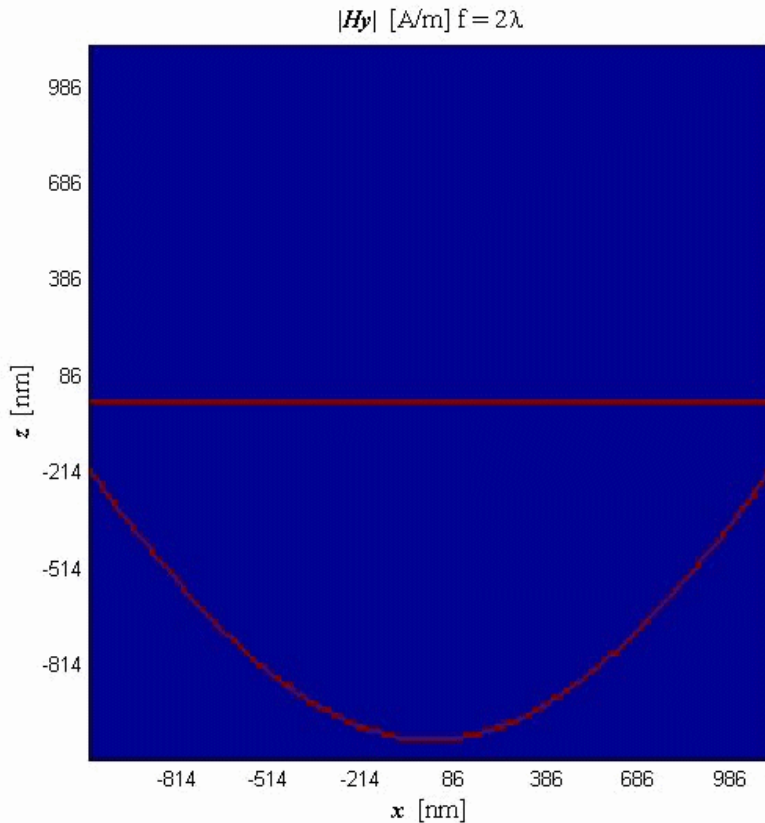
- S. C. Hagness, D. Rafizadeh, S. T. Ho, and A. Taflove, *IEEE J. Lightwave Tech.*, 1997.

- Lasing in a random clump of ZnO particles

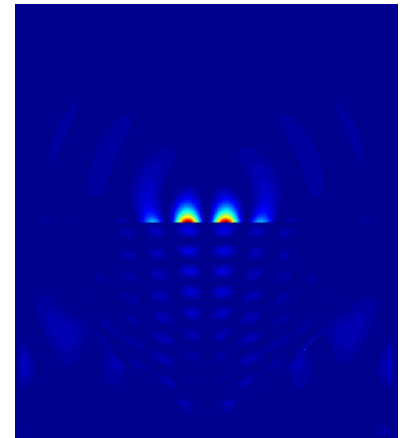
- H. Cao et al., *Phys. Rev. Lett.*, 2000.



Solid immersion lens simulation (FDTD)



Ex – component

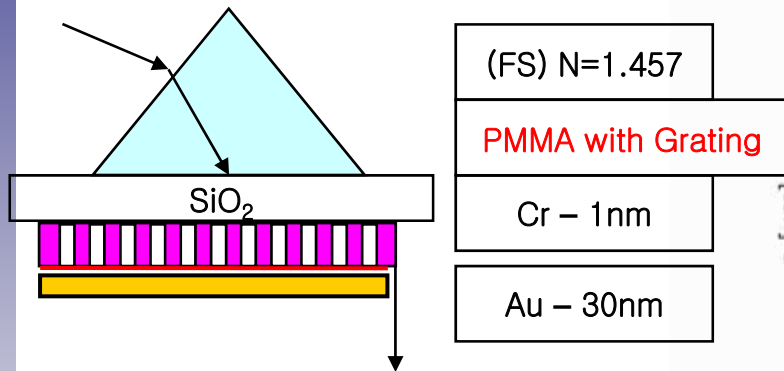


Ey – component

Extension to three-dimensional solid immersion lens nano-focusing for high density optical memory

FDTD example

Nd- YAG (532nm)



Lamella grating

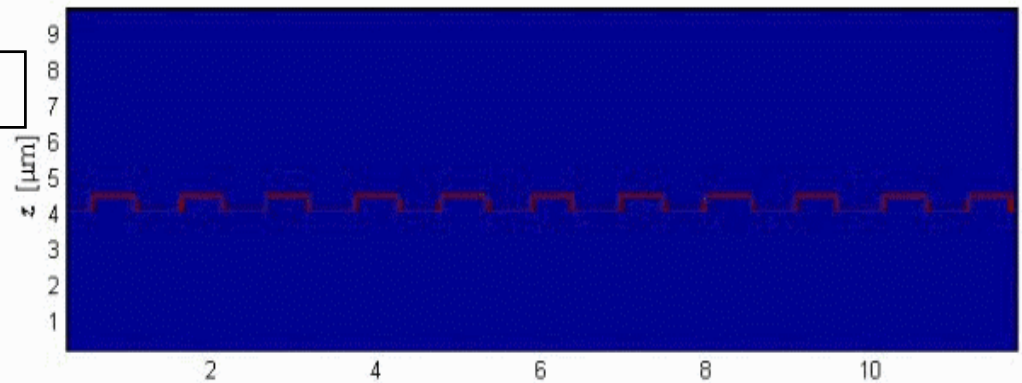
CASE 1



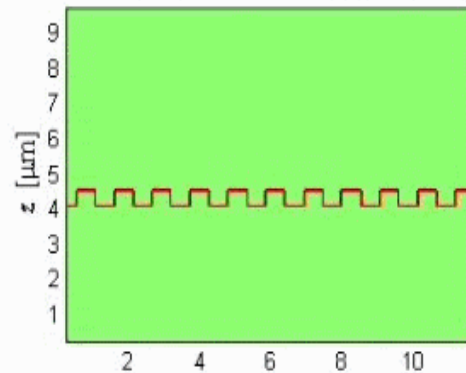
CASE 2



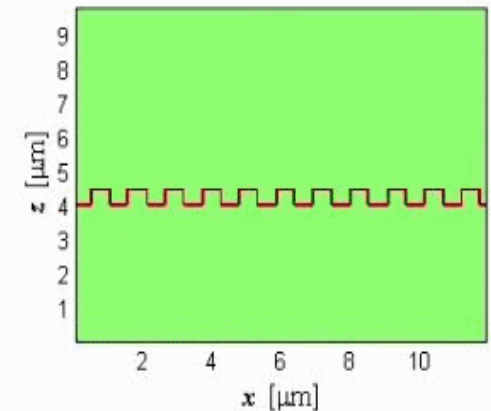
$|Hy|$ [A/m] with Au/PMMA 30nm & 450nm



E_x [V/m] with $\lambda = 532\text{nm}$ @ 43.9°



E_z [V/m] at $t = 3.33564 \times 10^{-16}$ [s]



Frequency domain method for the Maxwell equations

Homogeneous Maxwell equations in the spatial domain

$$\nabla \times \underline{E} = j\omega\mu_0\mu(x, y, z)(\hat{x}H_x + \hat{y}H_y + \hat{z}H_z)$$

$$\nabla \times \underline{H} = -j\omega\varepsilon_0\varepsilon(x, y, z)(\hat{x}E_x + \hat{y}E_y + \hat{z}E_z)$$

Fourier transform

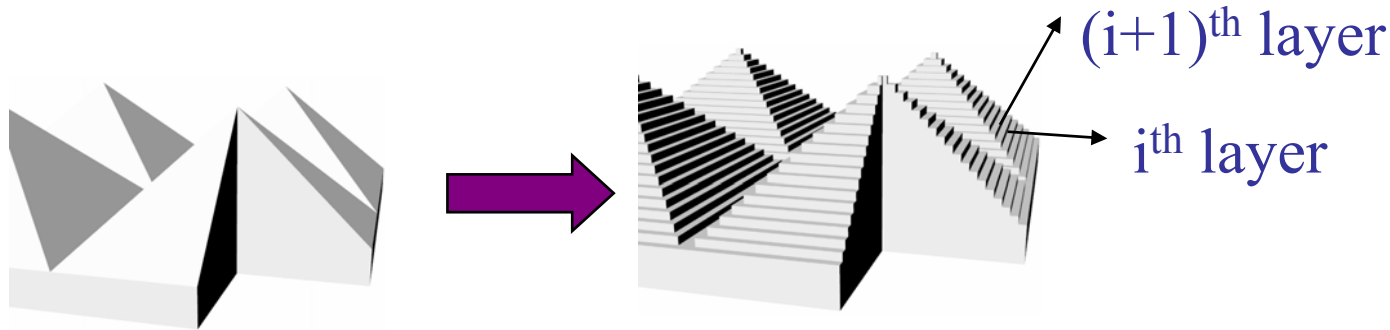
Homogeneous Maxwell equations in the (spatial) frequency domain

$$k_0 \begin{bmatrix} \underline{\varepsilon}_{(x)} & 0 & 0 & 0 & 0 & 0 \\ 0 & \underline{\varepsilon}_{(y)} & 0 & 0 & 0 & 0 \\ 0 & 0 & \underline{\varepsilon}_{(z)} & 0 & 0 & 0 \\ 0 & 0 & 0 & \underline{\mu}_{(x)} & 0 & 0 \\ 0 & 0 & 0 & 0 & \underline{\mu}_{(y)} & 0 \\ 0 & 0 & 0 & 0 & 0 & \underline{\mu}_{(z)} \end{bmatrix} \begin{bmatrix} \underline{E}_x \\ \underline{E}_y \\ \underline{E}_z \\ \underline{H}_x \\ \underline{H}_y \\ \underline{H}_z \end{bmatrix} = \begin{bmatrix} 0 & 0 & 0 & 0 & j\underline{K}_z & -j\underline{K}_y \\ 0 & 0 & 0 & -j\underline{K}_z & 0 & j\underline{K}_x \\ 0 & 0 & 0 & j\underline{K}_y & -j\underline{K}_x & 0 \\ 0 & j\underline{K}_z & -j\underline{K}_y & 0 & 0 & 0 \\ -j\underline{K}_z & 0 & j\underline{K}_x & 0 & 0 & 0 \\ j\underline{K}_y & -j\underline{K}_x & 0 & 0 & 0 & 0 \end{bmatrix} \begin{bmatrix} \underline{E}_x \\ \underline{E}_y \\ \underline{E}_z \\ \underline{H}_x \\ \underline{H}_y \\ \underline{H}_z \end{bmatrix}$$

The Maxwell equations in the spatial domain have partial differential operators. But Maxwell equations in the frequency domain are described by several algebraic equations.

Rigorous coupled wave analysis (RCWA)

Structure modeling (staircase approximation)



Fourier representation of the permittivity of the i^{th} layer

$$\varepsilon^{(i)}(x, y) = \sum_{g,h} \varepsilon_{gh}^{(i)} \exp[j(G_{x,g}x + G_{x,h}y)]$$

Fourier representation of the EM fields in the i^{th} layer

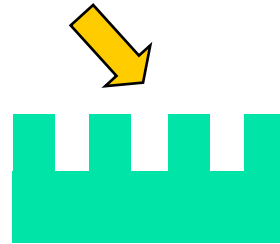
$$\underline{E}^{(i)} = \sum_{m=-M}^M \sum_{n=-N}^N \left[\underline{x}S_{x,mn}^{(i)}(z) + \underline{y}S_{y,mn}^{(i)}(z) + \underline{z}S_{z,mn}^{(i)}(z) \right] \exp[j(k_{x,m}x + k_{y,n}y)]$$

$$\underline{H}^{(i)} = j\sqrt{\frac{\varepsilon_0}{\mu_0}} \sum_{m=-M}^M \sum_{n=-N}^N \left[\underline{x}U_{x,mn}^{(i)}(z) + \underline{y}U_{y,mn}^{(i)}(z) + \underline{z}U_{z,mn}^{(i)}(z) \right] \exp[j(k_{x,m}x + k_{y,n}y)]$$

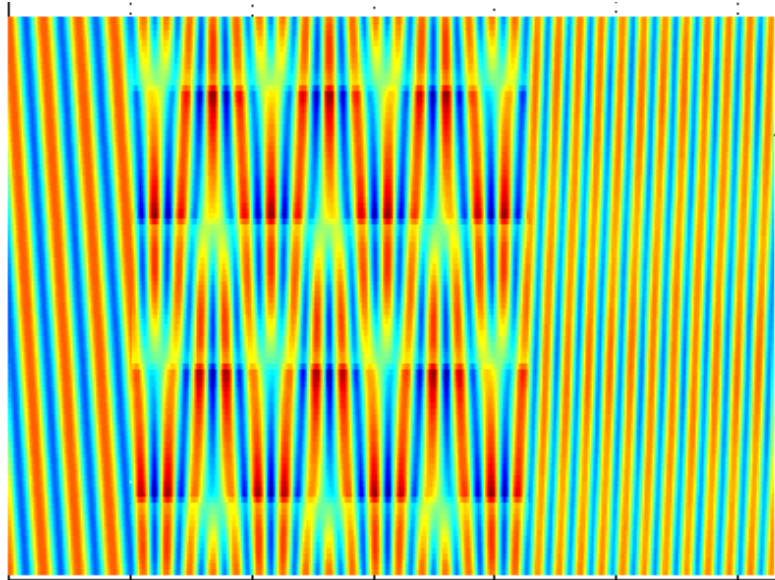
The boundary conditions between adjacent layers are satisfied by the S-matrix method.

RCWA examples

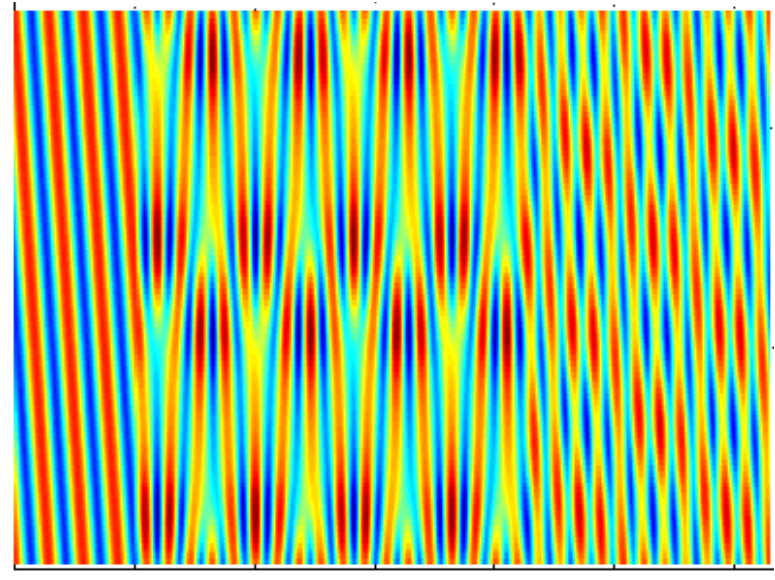
2D-binary dielectric grating showing polarization-dependent diffraction



TM-polarization



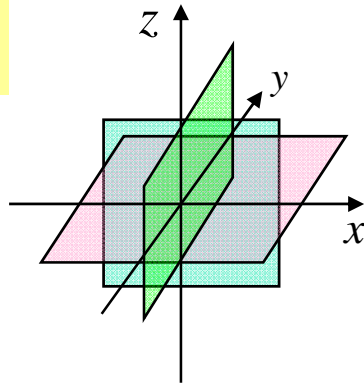
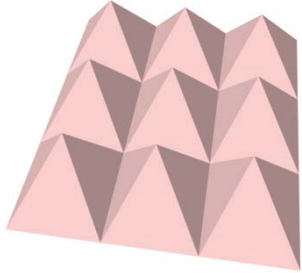
TE-polarization



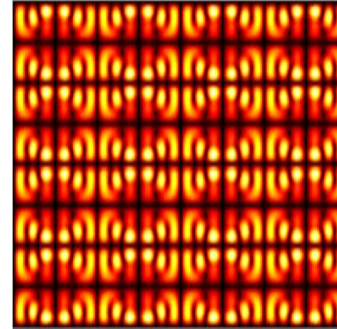
RCWA examples

3D micro-pyramid structure (15 level staircase approximation)

Wavelength(λ)=532nm
 Period= 3λ , Height= 6λ
 Normal incidence

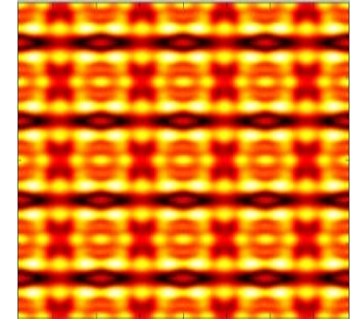


$|E_y|$



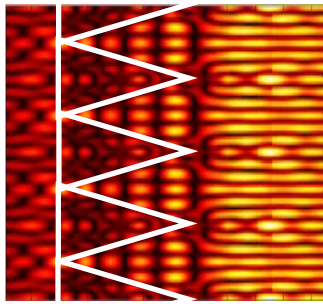
x-y crosssection

$|E_x|$



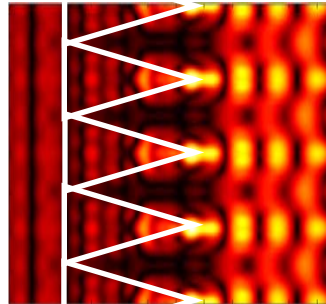
x-y crosssection

$|E_y|$



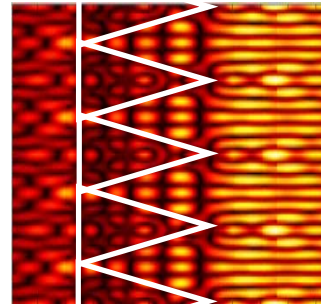
x-z crosssection

$|E_x|$



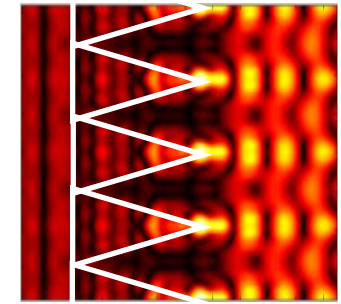
x-z crosssection

$|E_y|$



y-z crosssection

$|E_x|$



y-z crosssection

Pseudo-Fourier modal analysis (PFMA)

Structure modeling (3D Fourier series)



$$\varepsilon(x, y, z) = \sum_{s=-2M}^{2M} \sum_{t=-2N}^{2N} \sum_{p=-2H}^{2H} \tilde{\varepsilon}_{stp} \exp(j(k_{x,stp}x + k_{y,stp}y + k_{z,stp}z))$$

Pseudo-Fourier representation of the E-M field

$$\tilde{\mathbf{E}}_{\mathbf{k}} = e^{j(k_{x,0}x + k_{y,0}y + k_{z,0}z)} \sum_{m,n,q} (E_{x,m,n,q}\underline{x} + E_{y,m,n,q}\underline{y} + E_{z,m,n,q}\underline{z}) \exp(j(k_{x,mnq}x + k_{y,mnq}y + k_{z,mnq}z))$$

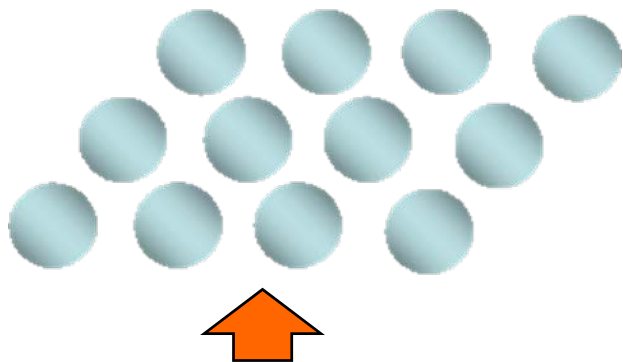
Maxwell equation in the PFMA

$$\begin{bmatrix} -j\underline{G}_z & 0 & \underline{K}_y \underline{\varepsilon}^{-1}(z) \underline{K}_x & \underline{\mu}_{(x)} - \underline{K}_y \underline{\varepsilon}^{-1}(z) \underline{K}_y \\ 0 & -j\underline{G}_z & -\underline{\mu}_{(y)} + \underline{K}_x \underline{\varepsilon}^{-1}(z) \underline{K}_x & -\underline{K}_x \underline{\varepsilon}^{-1}(z) \underline{K}_y \\ \underline{K}_y \underline{\mu}^{-1}(z) \underline{K}_x & \underline{\varepsilon}_{(x)} - \underline{K}_y \underline{\mu}^{-1}(z) \underline{K}_y & -j\underline{G}_z & 0 \\ -\underline{\varepsilon}_{(y)} + \underline{K}_x \underline{\mu}^{-1}(z) \underline{K}_x & -\underline{K}_x \underline{\mu}^{-1}(z) \underline{K}_y & 0 & -j\underline{G}_z \end{bmatrix} \begin{bmatrix} \underline{E}_y \\ \underline{E}_x \\ \underline{H}_y \\ \underline{H}_x \end{bmatrix} = \frac{jk_{z,0}}{k_0} \begin{bmatrix} \underline{E}_y \\ \underline{E}_x \\ \underline{H}_y \\ \underline{H}_x \end{bmatrix}$$

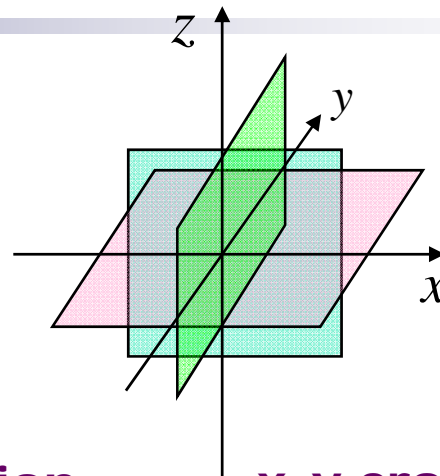
Eigenvalue

Eigenmode profile

Metallic micro structures

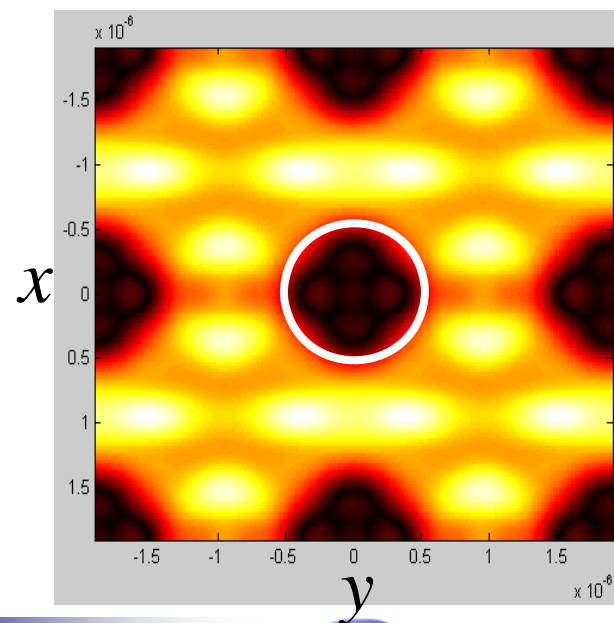
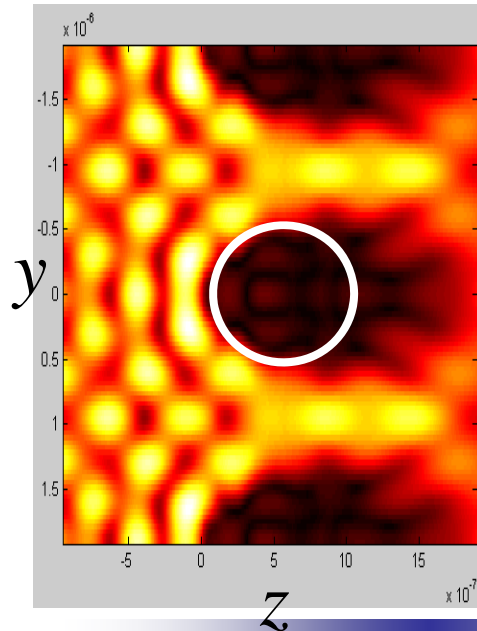
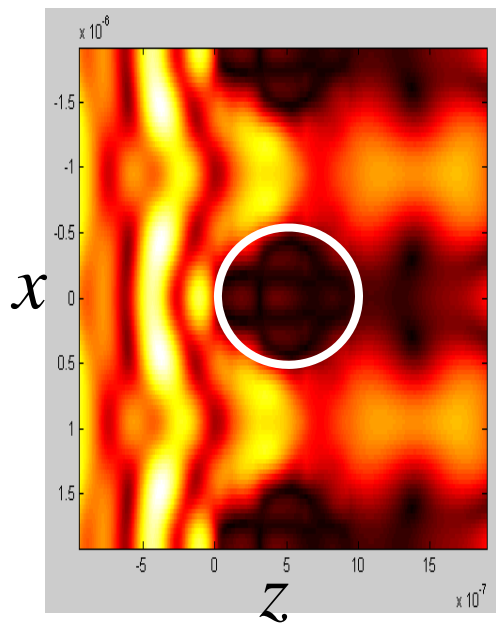


x-z crosssection



y-z crosssection

x-y crosssection

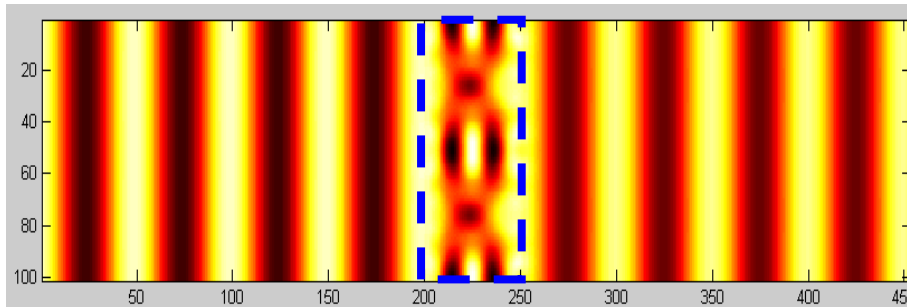
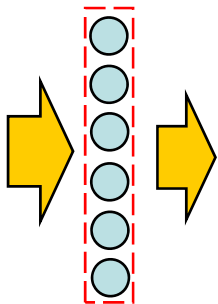


PFMA example

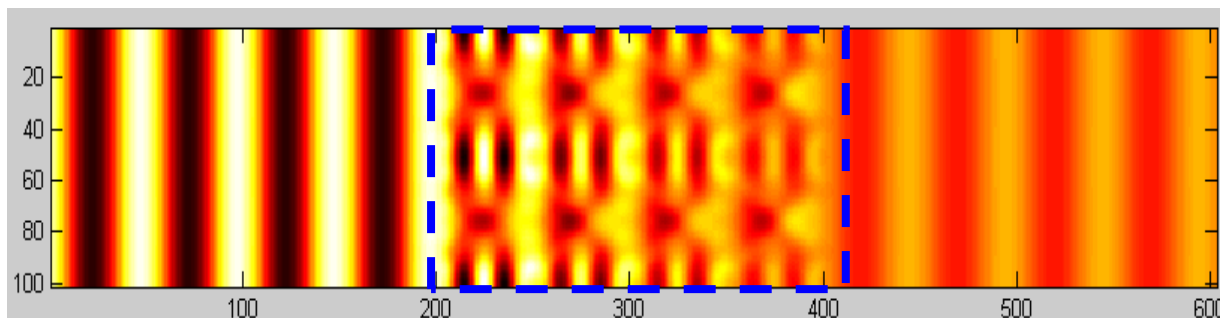
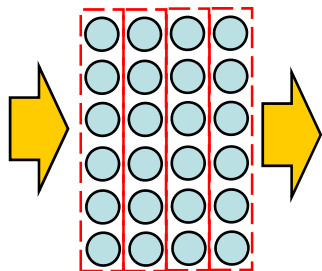
Longitudinally periodic and finite 2D photonic crystals

$$\mathbf{E} = \sum_g C_g \tilde{\mathbf{E}}_g$$

Total field distribution is a superposition of pseudo-Fourier eigenmodes with appropriate coupling coefficients.

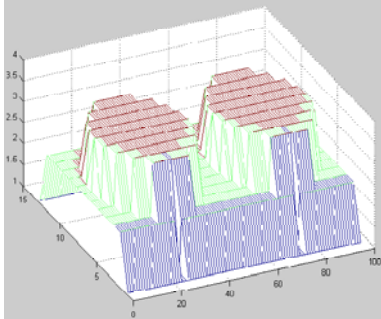


Wavelength(λ)=532nm
Period= 1.2λ , radius= 0.4λ
Normal incidence

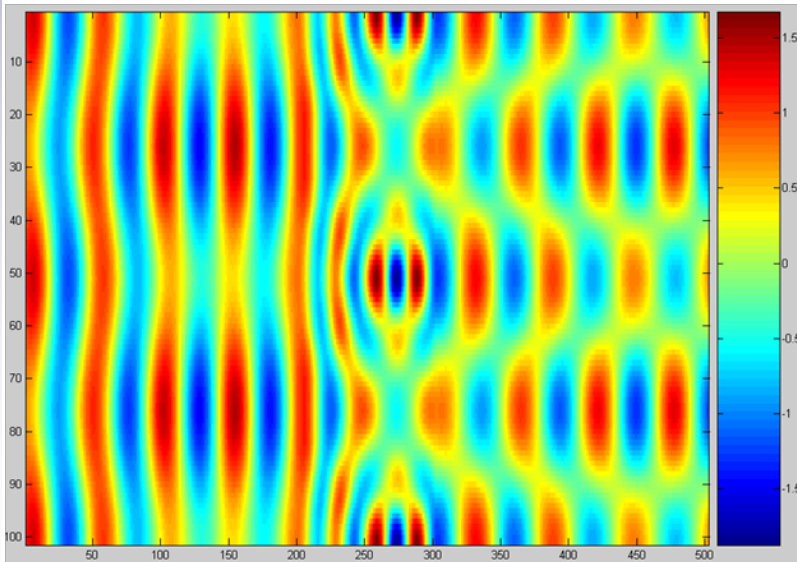


Bloch-eigen mode extraction in the PFMA

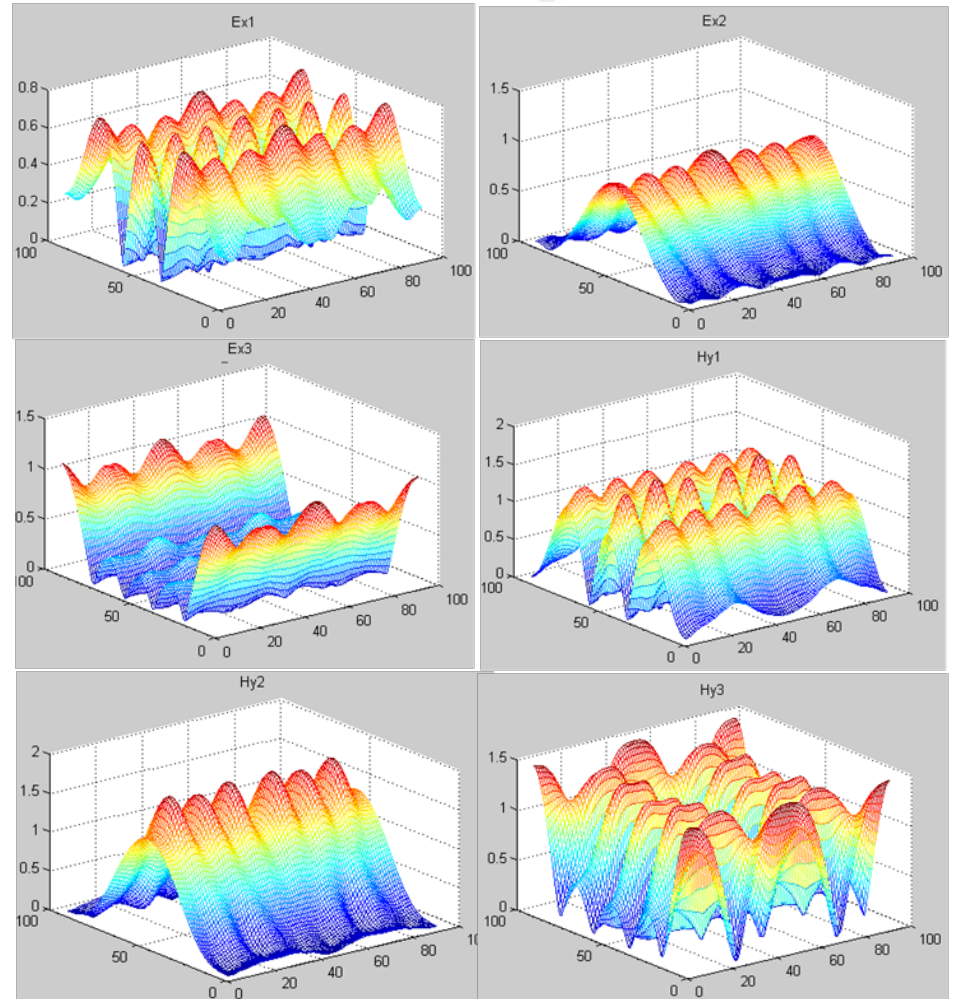
Analysis method:
Pseudo-Fourier modal analysis



Total E-field distribution



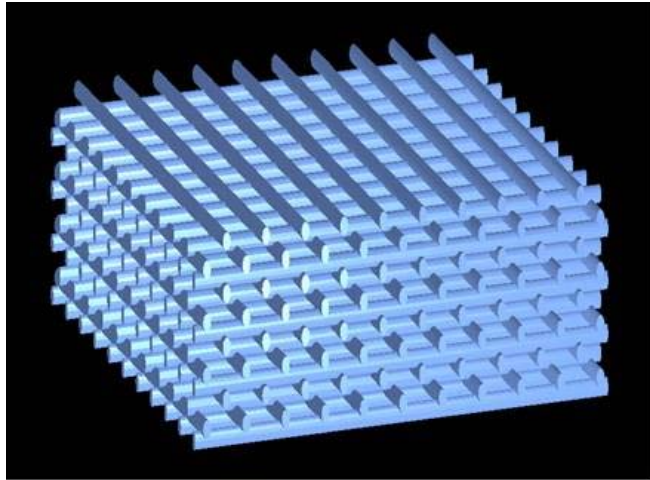
Extracted Bloch-eigenmodes



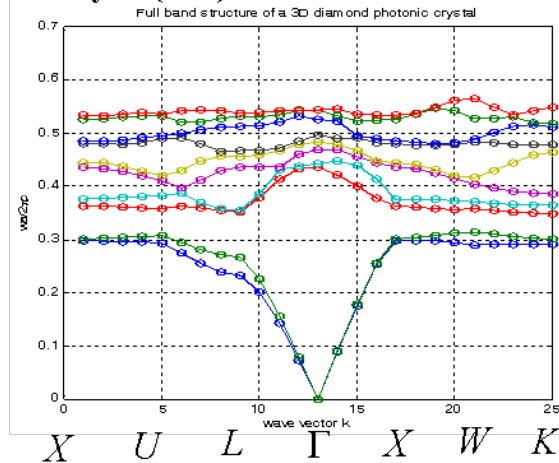
Comparison

	FDTD	RCWA	PFMA
Domain	Space	Frequency	Frequency
Field representation	Finite-difference method	Piles of truncated 2D-pseudo-Fourier series	Truncated 3D-pseudo-Fourier series
Structure modeling	Mesh-structure	Staircase approximation & piles of 2D-Fourier series	3D-Fourier series (no staircase approximation)
Aperiodic structure Analysis	Yes	No (If using PML, yes)	No (If using PML, yes)
Evanescent field analysis	No (Cannot separate)	Yes	Yes
Modal analysis	No	No	Yes
Computation cost	Very huge	Large	Huge

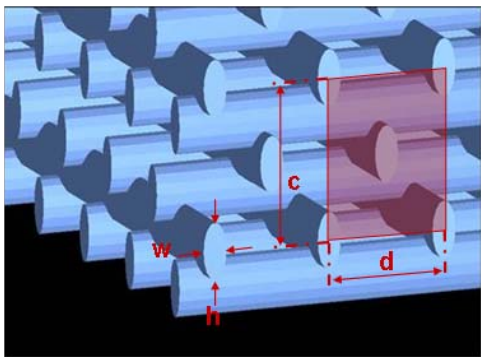
3D Photonic crystals



Full band structure of a woodpile photonic crystal (FCC) $n = 3.5$

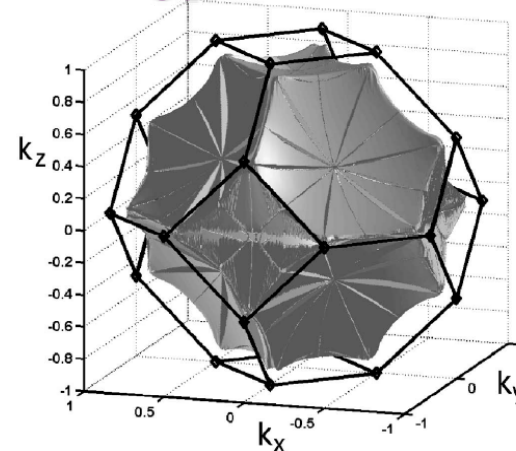


Photonic band structure calculation



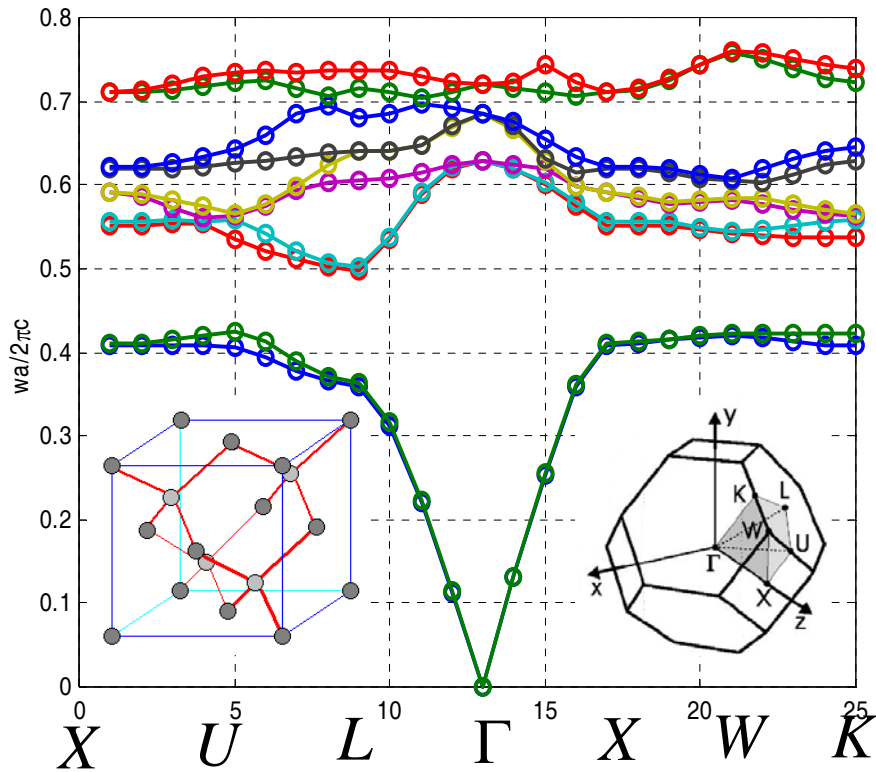
$$\begin{aligned} n &= 1.5 \\ w &= 0.3d \\ h &= 0.7d \\ c &= 2^{0.5}d \end{aligned}$$

Iso-energy surface calculation

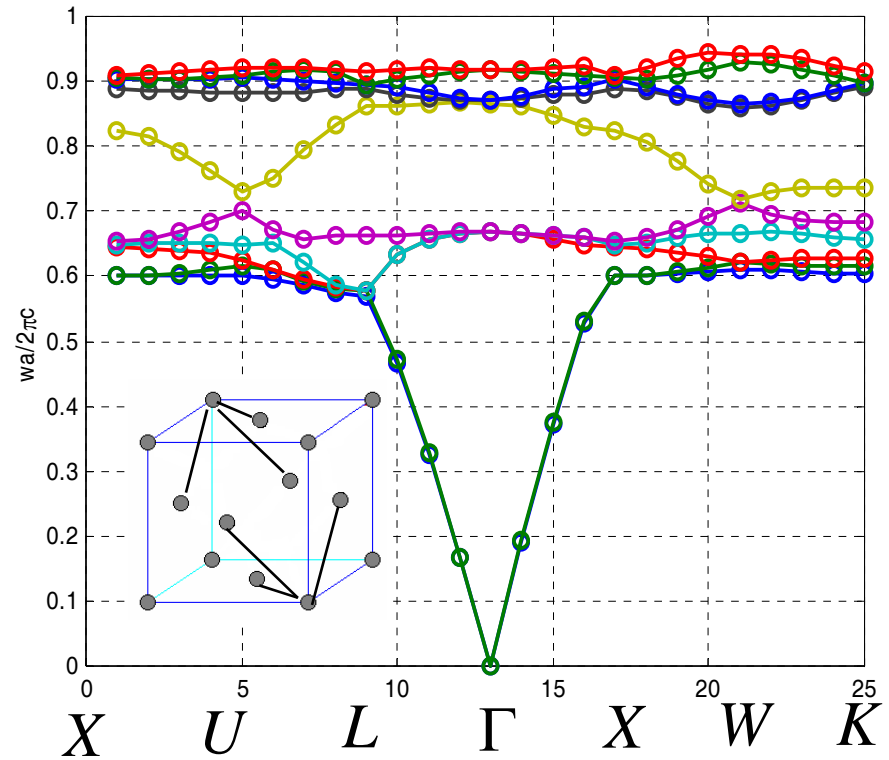


Examples

Full band structure of a 3D diamond photonic crystal (FCC) $n = 3.5$

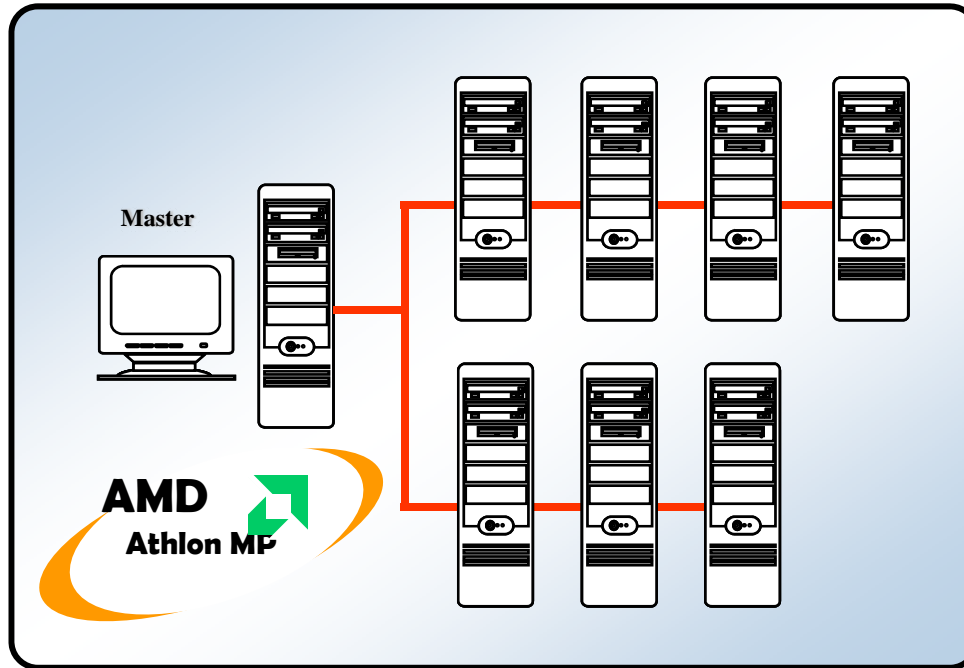


Full band structure of a 3D simple FCC photonic crystal $n = 3.5$



Perspectives : parallel computing

Parallel computing system



- ❑ Linux MPI 기반의 병렬 컴퓨터
- ❑ 16 × AMD MP 2000+ CPU의 병렬 시스템
- ❑ 16G RAM의 대용량 처리 가능
- ❑ 1Gbps의 초고속 분산 연결
- ❑ AMCL library for parallel matrix computation